Interactions with human blood in vitro and pharmacokinetic properties in mice of liposomal N4-octadecyl-1-beta-D-arabinofuranosylcytosine, a new anticancer drug

Koller-Lucae, S K ; Schott, H ; Schwendener, R

Abstract: The interactions of N4-octadecyl-1-beta-D-arabinofuranosylcytosine (NOAC), a lipophilic derivative of 1-beta-D-arabinofuranosylcytosine (ara-C), were studied in vitro with human blood components. Binding of NOAC incorporated into liposomes to erythrocytes (Ec) was saturated at 63 nmol/10(9) Ec and binding analysis resulted in a weak affinity of 3 x 10(3) liters/mol and 4 x 10(7) binding sites per Ec. The Ec partition coefficient D(Ec) was approximately 4, which demonstrates the high accumulation of NOAC in Ec membranes. The calculated fraction f(b) of drug bound to plasma proteins was 30%. Analysis of serum protein binding of NOAC was done by density gradient ultracentrifugation and agarose gel electrophoresis. Liposomal NOAC was distributed to low-density lipoproteins (LDL) at 36%, to high-density lipoproteins at 21%, to albumin and other proteins at 12% and to very-low-density lipoproteins at 5%. Comparable results were obtained for the analog N4-hexadecyl-1-beta-D-arabinofuranosylcytosine and when the drugs were dissolved in dimethyl sulfoxide. The biodistribution of liposomal NOAC in ICR mice after intravenous application revealed a biphasic blood concentration versus time curve with a distribution half-life t1/2alpha of 23 min and an elimination half-life t1/2beta of 7 h. The drug was distributed mainly into the liver with an organ load of 69% and with an elimination half-life of 8 h. The strong affinity of NOAC to LDL might be exploited for the enhanced uptake of the drug in tumor cells expressing high numbers of LDL receptor molecules.

0022-3565/97/2823-1572$03.00/0
THE JOURNAL OF PHARMACOLOGY AND EXPERIMENTAL THERAPEUTICS
JPET 282:1572–1580, 1997

Vol. 282, No. 3
Printed in U.S.A.

Interactions with Human Blood *in Vitro* and Pharmacokinetic Properties in Mice of Liposomal N^4-Octadecyl-1-β-D-arabinofuranosylcytosine, A New Anticancer Drug[1]

SIBYLLE K. M. KOLLER-LUCAE, HERBERT SCHOTT and RETO A. SCHWENDENER

Division of Cancer Research, Department of Pathology, University Hospital, Zürich, Switzerland (S.K.M.K.-L., R.A.S.) and Institute of Organic Chemistry, University of Tübingen, Germany (H.S.)

Accepted for publication May 14, 1997

ABSTRACT

The interactions of N^4-octadecyl-1-β-D-arabinofuranosylcytosine (NOAC), a lipophilic derivative of 1-β-D-arabinofuranosylcytosine (ara-C), were studied *in vitro* with human blood components. Binding of NOAC incorporated into liposomes to erythrocytes (Ec) was saturated at 63 nmol/10^9 Ec and binding analysis resulted in a weak affinity of 3×10^3 liters/mol and 4×10^7 binding sites per Ec. The Ec partition coefficient D_{Ec} was approximately 4, which demonstrates the high accumulation of NOAC in Ec membranes. The calculated fraction f_b of drug bound to plasma proteins was 30%. Analysis of serum protein binding of NOAC was done by density gradient ultracentrifugation and agarose gel electrophoresis. Liposomal NOAC was distributed to low-density lipoproteins (LDL) at 36%, to high-density lipoproteins at 21%, to albumin and other proteins at 12% and to very-low-density lipoproteins at 5%. Comparable results were obtained for the analog N^4-hexadecyl-1-β-D-arabinofuranosylcytosine and when the drugs were dissolved in dimethyl sulfoxide. The biodistribution of liposomal NOAC in ICR mice after intravenous application revealed a biphasic blood concentration *versus* time curve with a distribution half-life $t_{1/2\alpha}$ of 23 min and an elimination half-life $t_{1/2\beta}$ of 7 h. The drug was distributed mainly into the liver with an organ load of 69% and with an elimination half-life of 8 h. The strong affinity of NOAC to LDL might be exploited for the enhanced uptake of the drug in tumor cells expressing high numbers of LDL receptor molecules.

1-β-D-Arabinofuranosylcytosine is an effective chemotherapeutic agent for the treatment of acute myelogenous leukemia (Gahrton, 1983; Keating *et al.*, 1982; Plunkett and Gandhi, 1993). However, its usefulness is impaired by its rapid deamination to the biologically inactive metabolite ara-U (Ho and Frei, 1971). To increase the cytotoxic activity of ara-C numerous N^4-derivatives were synthesized to protect the drug from deamination and to alter its pharmacokinetic properties (Kanai and Ichino, 1974; Rosowsky *et al.*, 1982; Wempen *et al.*, 1968). Whereas short-chain modifications of ara-C at the N^4-amino group generally resulted in a weak enhancement of cytotoxicity (Aoshima *et al.*, 1976), lipophilic derivatives with long-chain fatty acids had a strong antitumor activity in murine tumor models (Kataoka and Sakurai, 1980; Tsuruo *et al.*, 1980). In a previous study, we reported that N^4-acyl derivatives of ara-C, incorporated into the membranes of small unilamellar liposomes, were active against murine L1210 leukemia and B16 melanoma at lower concentrations than unmodified ara-C (Rubas *et al.*, 1986). However, the protection against enzymatic deamination to ara-U was only partially achieved with the N^4-acyl derivatives. Therefore we synthesized the N^4-alkyl-ara-C derivatives NHAC and NOAC shown in figure 1 (Schwendener *et al.*, 1995a; Schwendener and Schott, 1992). These derivatives

Received for publication November 11, 1996.
[1] This work was supported by a grant from the E.G., G., G., and Ch. Sassella Foundation (to S.K.M.K.-L.) and in part by a grant from the Stiftung für angewandte Krebsforschung (to R.A.S.).

ABBREVIATIONS: ara-C, 1-β-D-Arabinofuranosylcytosine; ara-U, 1-β-D-arabinofuranosyluracil; NOAC, N^4-octadecyl-1-β-D-arabinofuranosylcytosine; NHAC, N^4-hexadecyl-1-β-D-arabinofuranosylcytosine; SPC, soy phosphatidylcholine; PB, phosphate buffer; saline/EDTA, saline containing 0.01% EDTA; DMSO, dimethyl sulfoxyde; EDTA, ethylenediaminetetraacetic acid; Ec, erythrocytes; B_{max}, maximal drug binding capacity; K_d, ligand concentration at half-maximal binding; r, binding rate; c_u, unbound drug; AEc, drug bound to Ec; Ec_{tot}, total concentration of Ec; D_{Ec}, Ec partition coefficient; A_{blood}, total drug in whole blood; A_{plasma}, drug in the plasma fraction; H, hematocrit; f_b, plasma protein-binding fraction; HDL, high-density lipoprotein; LDL, low-density lipoprotein; VLDL, very-low-density lipoprotein; KBr, potassium bromide; $t_{1/2\alpha}$, distribution half-life; $t_{1/2\beta}$, elimination half-life; $V_{d(area)}$, area-derived apparent volume of distribution; V_c, apparent volume of the central compartment; V_p, apparent volume of the peripheral compartment; Cl_{total}, systemic clearance; $AUC_{(tr.\ 0 \rightarrow \infty)}$, area under the curve for time zero to infinity calculated model-independently with the trapezoidal rule; AUMC, area under the moment curve; c_{blood}, drug concentration in blood; c_{plasma}, drug concentration in plasma; V_{blood}, total blood volume; MRT, mean residence time; Cl_{in}, tissue uptake rate index; $T(t_1)$, amount of drug in the tissue at time t_1; Cl_{organ}, organ clearance; W_{organ}, organ weight; HPLC, high-performance liquid chromatography.

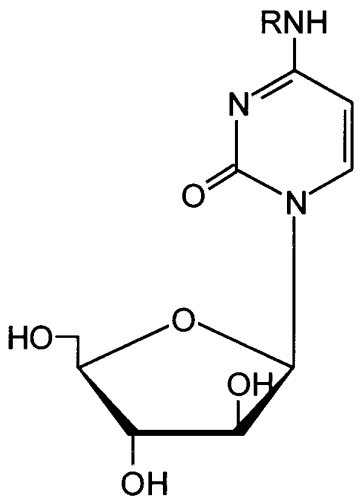

	R	Molecular weight
ara-C	H	243.2
NOAC	$C_{18}H_{37}$	495.7
NHAC	$C_{16}H_{33}$	467.7

Fig. 1. Chemical structures of ara-C, NOAC and NHAC.

were found to be extremely resistant toward deamination in plasma as well as in the liver (Schwendener *et al.*, 1995b). Because of the very low solubility in aqueous media NHAC and NOAC were incorporated into the lipid membranes of small unilamellar liposomes to allow their parenteral application. Liposomal preparations of NHAC and NOAC exerted significantly higher cytotoxic activities in the L1210 leukemia model than ara-C. In contrast to the parent drug and to some other lipophilic ara-C derivatives, NHAC and NOAC were found to exert excellent antitumor effects after oral therapy (Schwendener *et al.*, 1996; Schwendener and Schott, 1996). We conclude from these and the following findings that the mechanisms of action of the N^4-alkyl-ara-C derivatives are different from ara-C. Their cellular uptake is nucleoside-transporter independent and only 2 to 5% were phosphorylated to ara-C triphosphate in HL-60, K-562 and U-937 cells (Horber *et al.*, 1995b, c). The cytotoxicity of NHAC was found to be less S-phase specific than ara-C, and induction of apoptosis occurred only at very high drug concentrations (Horber *et al.*, 1995d). Presently, we concentrate our studies on NOAC because this derivative has the highest antitumor activity of all N^4-alkyl analogs (Schwendener *et al.*, 1995a). A phase I/II study of liposomal NOAC is currently underway at the University Hospital Zurich.

It is known that single-chain acyl compounds like fatty acids are not tightly anchored within the lipid bilayer of liposomes and that they are readily transferred to plasma proteins and Ec membranes (Kamp *et al.*, 1993; Kleinfeld and Storch, 1993; Richieri *et al.*, 1993). We assumed that the N^4-alkyl-ara-C derivatives, which have no amphiphilic properties and are not charged at physiological pH, move through lipid membranes of the liposomes and are transferred to blood components at rates that are comparable with long-chain fatty acids.

Therefore, in this report we investigated the interactions of NOAC with human blood *in vitro* and compared them with the properties of NHAC. Ec binding was measured and protein binding was calculated with the Ec partition coefficient D_{Ec}. In addition, we studied the distribution of the drugs between the serum lipoproteins which were separated by ultracentrifugation on a KBr density gradient and analyzed on agarose gels. In the second part of this contribution we determined the blood and organ distribution *in vivo* of liposomal NOAC in ICR mice and calculated the pharmacokinetic parameters.

Methods

Chemicals. NHAC and NOAC were synthesized as described previously (fig. 1; Schwendener *et al.*, 1995a; Schwendener and Schott, 1992). SPC was obtained from L. Meyer, Hamburg, Germany. Cholesterol (Fluka AG, Buchs, Switzerland) was recrystallized from methanol. DL-α-Tocopherol and all analytical grade buffer salts and other chemicals used were from Merck, Darmstadt, Germany or Fluka, Buchs, Switzerland. NHAC and NOAC were tritium labeled (0.189 Gbq/mmol [5-^{3}H]NHAC and 0.370 Gbq/mmol [5-^{3}H]NOAC) by Amersham Int., Amersham, UK. Soluene 350 and Ultima Gold scintillation cocktail were from Packard Instruments, Groningen, The Netherlands.

Preparation of liposomes. Small unilamellar liposomes were prepared by sequential filter extrusion of multilamellar liposomal preparations through Nuclepore membranes (Sterico, Dietikon, Switzerland) of 0.4 μm, 0.2 μm and 0.1 μm pore diameter with a Lipex extruder (Lipex Biomembranes Inc., Vancouver, Canada; Hope *et al.*, 1985). For experiments with human blood or intravenous injection into mice, liposomes were either prepared in PB (67 mM, pH 7.4) or in saline, containing 0.01% EDTA (saline/EDTA) for the incubations with serum. Liposome size and homogeneity were determined by laser light scattering (Submicron Particle Sizer Model 370, Nicomp, Santa Barbara, CA). The basic lipid composition of the liposomes used for *in vitro* incubations with blood and serum was 40 mg/ml SPC, 4 mg/ml cholesterol, 0.2 mg/ml DL-α-tocopherol and 2.5 mg/ml of the drugs NOAC or NHAC, whereas the liposomes used for the pharmacokinetic experiments were composed of 80 mg/ml SPC, 8 mg/ml cholesterol, 0.4 mg/ml DL-α-tocopherol and 11 mg/ml NOAC. All preparations were trace labeled with [5-^{3}H]NOAC or [5-^{3}H]NHAC, respectively, sterile filtrated (0.2 μm, Schleicher & Schuell, Dassel, Germany), stored at 4°C and used within 3 days after preparation. For control experiments stock solutions of NHAC and NOAC (2.5 mg/ml, corresponding to their highest stable solubility) in DMSO were prepared.

***In vitro* distribution of NOAC and NHAC in human blood.** Fresh venous blood was collected in EDTA tubes (Vacutainer, Becton Dickinson, Meylon Cedex, France) from a healthy donor after an overnight fast. For the incubation experiments, 1.5 ml blood containing $6 \pm 1 \times 10^9$ Ec (hematocrit, 0.3–0.4) were spiked either with the drugs in liposomes or in DMSO to yield final drug concentrations of 60 to 1100 μM (liposomes) or 100 and 200 μM (DMSO) in a total volume of 2 ml. After incubation on a blood sample shaker (Specimix, Bioblock, Frenkendorf, Switzerland) for 4 h at 37°C the blood samples were centrifuged (10 min, $650 \times g$, 20°C) and plasma was removed. The blood cells were not separated further, because as

shown before with NHAC, binding to leukocytes was negligible (approximately 2%; Horber *et al.*, 1995a). Thus, the whole-blood cell fraction was referred to as Ec. The Ec samples were washed three times with PB, centrifuged (10 min, 650 × *g*, 20°C) and then solubilized, and the [5-^{3}H]NOAC or [5-^{3}H]NHAC activity was detected by scintillation counting as described previously (Horber *et al.*, 1995a). All experiments were carried out in triplicate. To exclude the possibility of precipitation of NOAC dissolved in DMSO in these incubations, the following control experiments in diluted serum were performed. The ^{3}H-labeled drug dissolved in 50 μl DMSO (0.28 mM final concentration) was incubated in 450 μl serum diluted with 500 μl saline/EDTA for 4 h at 37°C. The serum was centrifuged (650 × *g*, 10 min) and the [5-^{3}H]NOAC concentration was determined in the supernatants. Corresponding controls were made by use of saline/EDTA instead of serum.

Analysis of binding parameters. To fit the concentration-dependent binding curve of NOAC and NHAC to Ec we used a one-site binding model:

$$y(x) = \frac{B_{max}x}{K_d + x} \quad (1)$$

with B_{max}, maximal binding capacity, and K_d, concentration of the ligand to determine half-maximal binding. The binding parameters of the two drugs to Ec were calculated from linearized curves of the binding rate r given in equation 2 *versus* unbound drug c_u.

$$r = \frac{[AEc]}{[Ec_{tot}]} \quad (2)$$

with [AEc], drug bound to Ec in millimolar (corresponding to 6.022 × 10^{20} Ec per liter) and [Ec_{tot}], total concentration of Ec in millimolar. The Ec partition coefficient D_{Ec} was calculated according to equation 3:

$$D_{Ec} = \frac{(A_{blood} - A_{plasma})(1 - H)}{HA_{plasma}} \quad (3)$$

with A_{blood}, the absolute amount of drug in whole blood (nanomoles); A_{plasma}, drug in the plasma fraction (nanomoles) and H, hematocrit (Derendorf and Garrett, 1983). The plasma protein-binding fraction f_b was determined from D_{Ec} as described in equation 4:

$$f_b = 1 - \frac{A_{blood} - c_{plasma}V_{blood}(1 - H)}{D_{Ec}c_{plasma}V_{blood}(1 - H)}\left(\frac{1}{H} - 1\right) \quad (4)$$

with c_{plasma}, concentration in the plasma fraction of the probe, and V_{blood}, the volume of whole blood.

***In vitro* distribution of NOAC and NHAC in human serum.** Fresh serum with normal cholesterol and lipoprotein levels was obtained from a healthy donor after overnight fasting. The blood was allowed to coagulate for 2 h and then centrifuged (10 min, 650 × *g*, 20°C). The drugs (0.1 ml; final concentration, 200 μM) were added either as liposomal preparation or dissolved in DMSO to 0.9 ml serum corresponding to the serum contained in 1.5 ml whole blood. After incubation for 4 h at 37°C on a blood sample shaker the separation of the plasma proteins was performed by gradient ultracentrifugation according to Chapman *et al.* (1981) and Redgrave *et al.* (1975) with small modifications. A density gradient was formed in ultracentrifuge tubes (Polyallomer, 5 ml, Beckman, Geneva, Switzerland) by adding 0.325 g KBr to 1 ml of the serum supernatants ($d_{20}{}^{20}$ 1.21), which were overlaid sequentially with solutions of 1 ml KBr in saline of the decreasing densities $d_{20}{}^{20}$ 1.064, 1.020 and 1.007. Finally, 1 ml of distilled water was added on top. The probes containing the drugs in liposomes or in DMSO and the appropriate controls replacing the serum with saline/EDTA and serum alone (fig. 3) were placed in a SW 50.1 rotor (Beckman, Geneva, Switzerland) and centrifuged for 22 h at 300,000 × *g* and 15°C in an ultracentrifuge (Centrikon T-1065, Kontron Instruments, Zürich, Switzerland). After careful removal of the tubes from the rotor a fine glass capillary was gently immersed to the bottom of each tube and 50 fractions of 0.17 ml were collected with a fraction collector (Superrac LKB, Uppsala, Sweden). Protein absorption was monitored continuously with a flow detector (Uvicord SII, LKB) at 279 nm. Drug concentration per fraction and initial concentration of the probes were analyzed by scintillation counting. The densities of the KBr solutions and of the individual fractions after centrifugation were determined with a densitometer (DMA 38, Anton Paar KG, Graz, Austria). All incubations were carried out in triplicate. The separation of the lipoproteins was controlled by electrophoresis on 1% agarose gels by a modified method described by Nobel (1968). From each centrifuged serum fraction an aliquot prestained with Sudan black B was applied to the gels. To provide further evidence of the transfer of liposomal NOAC to the lipoproteins, selected HDL- and LDL-rich fractions from the KBr gradient separation (*cf.* fig. 3) were run on a gel (*cf.* inset, fig. 4), and the bands corresponding to HDL or LDL were cut and analyzed for [5-^{3}H]NOAC activity (*cf.* curves in fig. 4).

NOAC pharmacokinetics and organ distribution in mice. Female mice (ICR, 27–38 g) were injected intravenously in the tail vein with 2.3 mg (4.6 μmol) liposomal NOAC in a volume of 200 μl. After periods ranging from 4 min to 24 h groups of three mice were sacrificed and blood, liver, spleen, kidneys, lung and brain were collected. To determine the concentration of NOAC in blood and the organs the samples were solubilized and further treated as described previously (Horber *et al.*, 1995a). Drug concentrations in organs were corrected for the remaining blood (Allen, 1989). All values for blood and organ distribution (figs. 5 and 6) were standardized with the body weight of a mouse of 20 g and given as percent of disintegrations per min injected per ml blood or as percent of disintegrations per min injected per total organ.

Pharmacokinetic analysis. The blood concentration *versus* time curve (fig. 5A) was approximated by the residual method which led to equation 5 of a two-compartment open model for intravenous drug application. The calculated parameters A, B, α and β of equation 5 were used to fit the curve:

$$y = Ae^{-\alpha t} + Be^{-\beta t} \quad (5)$$

where (A + B), peak drug concentration in blood at time t = 0 min. The distribution $t_{1/2\alpha}$ and elimination $t_{1/2\beta}$ half-lives were calculated from the slopes α and β. The apparent volume of distribution $V_{d(area)}$, the apparent volume of the central V_c and peripheral V_p compartments, the systemic clearance Cl_{total} were calculated by equations described elsewhere (Greenblatt and Koch-Weser, 1975). The area under the curve for time zero to infinity $AUC_{(tr.\ 0\to\infty)}$ was calculated model-independently with the trapezoidal rule to the last measured time point t = 1440 min and extrapolation to infinity ($c_{blood(1440\ min)}$ divided by β). To compare the organ load of the different organs, the percentage of the organ $AUC_{(tr.\ 0\to\infty)}$ was compared with the sum of all organ $AUC_{(tr.\ 0\to\infty)}$ values. The organ load is a measure of how much drug ever appears in one organ during the whole period between application and total elimination of the drug. The AUMC was calculated with equation 6.

$$AUMC = \int_0^\infty tc_{blood}dt \quad (6)$$

with the drug concentration in blood (c_{blood}). The MRT was calculated by dividing the AUMC with the $AUC_{(tr.\ 0\to\infty)}$.

As relative peak concentrations of NOAC in the mouse organs the time point with highest measured drug concentration in the particular organ was considered (table 2). Further data analysis as described by Nishikawa *et al.* (1993) for ara-C made it possible to

calculate the different organ clearances and the total clearance by use of the tissue uptake rate index Cl_{in}.

$$Cl_{in} = \frac{T(t_1)}{\int_0^{t_1} c_{blood}(t)dt} = \frac{T(t_1)}{\int_0^{t_1} T(t_1)/AUC_{0\rightarrow t_1}} \quad (7)$$

with $T(t_1)$, amount of drug in the tissue at time t_1 and $AUC_{(0\rightarrow t_1)}$, area under the blood concentration *versus* time ($t_0 \rightarrow t_1$) curve. The organ clearance Cl_{organ} is given by

$$Cl_{organ} = Cl_{in} W_{organ} \quad (8)$$

with W_{organ}, organ weight in grams. To be able to compare our data with the results of Nishikawa *et al.* (1993), our data were normalized to mice of 26.5 g average body weight, and drug concentrations at 120 min were extrapolated from the blood *versus* time curve and the organ concentration *versus* time curve.

Results

Concentration-dependent binding of NOAC and NHAC to Ec. The binding curves of liposomal NOAC and NHAC to Ec are shown in figure 2. The data were fitted with a one-site binding model described by equation 1, which results in saturation values of 63 nmol/10^9 Ec for NOAC and 88 nmol/10^9 Ec for NHAC, respectively. Saturation is reached by use of at least 0.7 mM NOAC or 0.9 mM NHAC under the experimental conditions. A significant difference in the binding to Ec between NOAC and NHAC was found only above saturation (P = .033, Student's *t*-test, fig. 2). Linearization of *r versus* c_u according to Lineweaver-Burk (correlation coefficient r = 0.963 for NOAC and 0.992 for NHAC) or Scatchard plots (r = 0.869 for NOAC and 0.987 for NHAC) resulted in 4 × 10^7 binding sites per Ec for NOAC and 5 × 10^7 for NHAC with a low binding affinity of 3 × 10^3 liters/mol for both drugs. The Ec partition coefficient D_{Ec} calculated after equation 3 was determined with the drugs (0.1 and 0.2 mM) dissolved in DMSO to avoid possible interference of the liposomal lipids with the binding of the drugs to Ec membranes. The altered drug formulation did not affect the binding characteristics of the drugs to Ec (fig. 2). For NOAC at 0.1 and 0.2 mM, a D_{Ec} of 4.2 ± 0.4 resulted, whereas for NHAC the D_{Ec} was 3.0 ± 0.4 (significant difference, P = .0004). According to equation 4, the fraction of drug bound to plasma proteins f_b, which was calculated with the D_{Ec} values, was 32 ± 3% for NOAC and 35 ± 5% for NHAC, which were not significantly different (P = .236).

To exclude the possibility of the formation of drug precipitates in the Ec fraction, control incubations in serum with ^{3}H-labeled NOAC dissolved in DMSO (0.28 mM incubated with diluted serum) showed that 100 ± 2% of the drug was dissolved in the serum, and that despite the low solubility of NOAC, no precipitates or crystals were found by microscopic observation. Identical results were obtained with liposomal NOAC at 1.1 mM, whereas in serum-free controls where the drug was dissolved in DMSO, 80 to 90% of NOAC was precipitated.

Binding of NOAC to serum proteins. To further characterize the binding properties of NOAC to serum proteins, the drug was incubated (4 h, 37°C) with fresh human serum, followed by separation of the proteins on a KBr density gradient. To monitor the gradient after ultracentrifugation a control run with saline/EDTA was performed and the densities of the fractions were determined. As shown in figure 3 the discontinuous gradient was smoothed after centrifugation. The separation of the lipoproteins was confirmed by agarose gel electrophoresis of all collected serum fractions

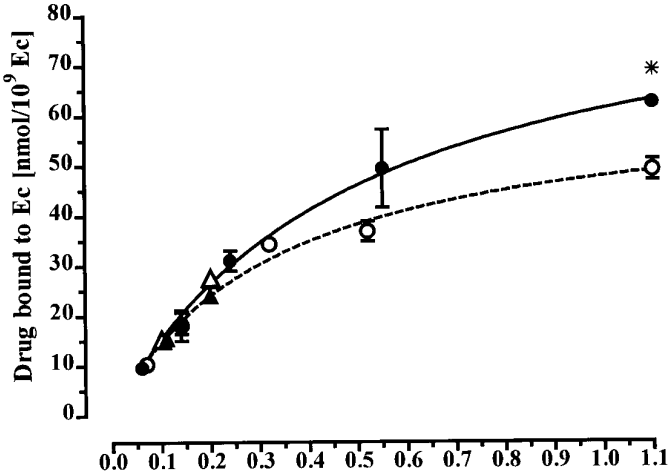

Fig. 2. Binding curves of NOAC (○) and NHAC (●) in liposomes (0.06–1.1 mM) to Ec determined as described under "Methods." For a comparison, the binding of NOAC (△) and NHAC (▲) dissolved in DMSO (0.1 and 0.2 mM) was determined under the same conditions. Drug concentration in Ec was determined by scintillation counting. Only the values at 1.1 mM were significantly different (*P = .033; Student's *t*-test). The fit with a one-site binding model (equation 1) resulted in saturation values of 63 nmol/10^9 Ec for NOAC (correlation coefficient, r = 0.930) and 88 nmol/10^9 Ec for NHAC (r = 0.997). Each point represents the mean ± S.D. of three measurements. Invisible error bars are smaller than the symbols.

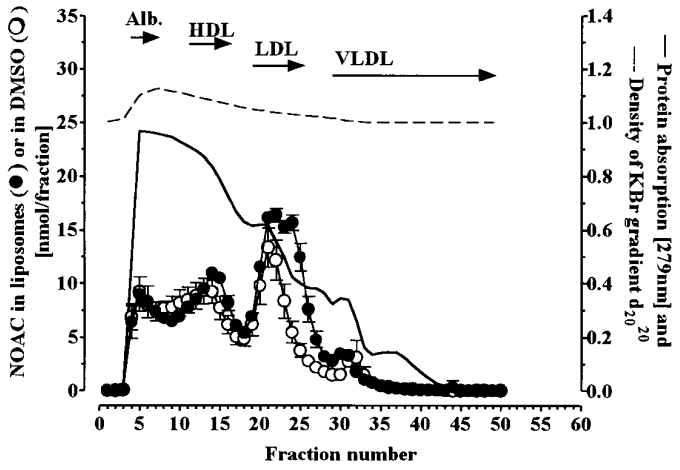

Fig. 3. Distribution of NOAC (250 μM) in liposomes (●) and DMSO (○) after incubation with human serum (4 h, 37°C) and gradient ultracentrifugation over a KBr gradient (d_{20}^{20} 1.21, 1.064, 1.020, 1.007, 1.000; centrifuged 22 h, 300,000 × *g*, 15°C), collection of fractions (0.17 ml) and scintillation counting for 5-^{3}H-labeled drug activity. Control serum (full line) was treated as described above and the proteins were monitored by UV-spectroscopy (λ_{279nm}). Fractions were pooled for albumin (fractions 4–7), HDL (fractions 11–16), LDL (fractions 19–25) and VLDL (fractions 29–50), and the concentrations of bound drug were calculated. Additionally, the equilibrated density gradient (dashed line) given in d_{20}^{20} after centrifugation was superimposed. Data are means of triplicates. A comparable distribution was obtained with NHAC (not shown). Alb., albumin.

(data not shown). Lipoprotein-containing fractions were pooled according to their densities and agarose gel patterns (*cf.* table 1). The centrifuge tubes showed the typical density bands where the corresponding lipoproteins were expected (Chapman *et al.*, 1981; Redgrave *et al.*, 1975). Additionally, a white band with liposomes was detected in the density range of $d_{20}{}^{20}$ 1.063 to 1.019, close above the LDL band. The diameters of the liposomes used ranged from 30 to 80 nm and their density was similar to that of LDL. Therefore, it was not possible to separate them clearly from LDL. Control centrifugations containing NOAC in DMSO and with substitution of serum by saline/EDTA resulted in a different distribution pattern with most of the drug accumulated at $d_{20}{}^{20}$ 1.1034, corresponding to the density of the solvent DMSO. This formulation was used to document the binding properties of the drug to LDL without interference of the liposomal carriers because only drug bound to LDL appeared in fractions 19 to 25. This experiment resulted in a similar distribution pattern as obtained with liposomal NOAC (fig. 3). With NHAC comparable patterns of distribution were found for all incubations (data not shown).

In table 1 the results of the serum protein distribution of NOAC are compared with NHAC. The highest distribution of liposomal NOAC was determined in LDL with 35.7 ± 1.0%. NHAC binding to LDL under equal conditions was 29.8 ± 0.9% and significantly lower than NOAC (P = .0016).

There was also a significant difference between the two formulations for the drugs bound to the HDL fraction for NOAC (P = .0412) and to the LDL fraction for NHAC (P = .0002) caused by the nature of the preparations (*cf.* table 1). However, because there was no significant difference between the binding of NOAC to LDL when applied in liposomes or DMSO, we assume that the transfer of NOAC to LDL is not impeded by the liposomes.

Further evidence that the liposomes do not retain NOAC from the interaction with LDL is shown in figure 4. Fractions rich in LDL had [5-^{3}H]NOAC activity in the LDL band after separation by agarose gel electrophoresis. This activity resulted from drug bound to LDL because liposomes do not run on agarose gels (data not shown). Similarly, the fractions rich in HDL contained [5-^{3}H]NOAC in the corresponding HDL band. No radioactivity was detected in LDL-free bands (fractions 6, 8, 13) and with the decreasing HDL concentrations in the following fractions, the NOAC concentration detected in these bands was reduced.

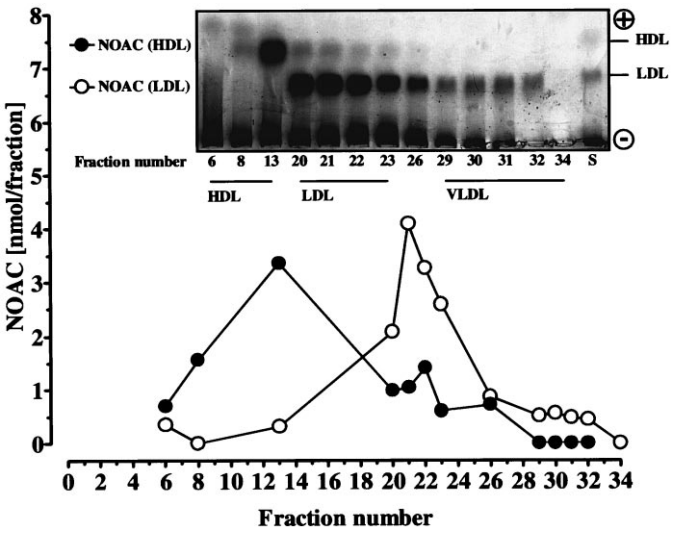

Fig. 4. Binding of NOAC to HDL (●) and LDL (○). Representative fractions containing the lipoproteins from figure 3 were prestained with Sudan black B and run on a 1% agarose gel (inset). The [5-^{3}H]NOAC concentration was determined by cutting out the corresponding bands (graph). S, diluted serum (1:20, v/v).

Pharmacokinetics of NOAC in mice. The NOAC kinetic values in female ICR mice were determined after intravenous injection of NOAC and the sacrifice of groups of three mice at adequate time points. The blood concentration *versus* time curve is biphasic, yielding a distribution half-life $t_{1/2\alpha}$ of 23 min and an elimination half-life $t_{1/2\beta}$ of 7 h (fig. 5A). As comparison, the elimination half-life $t_{1/2\beta}$ of ara-C was found to be 21 min after i.p. administration in mice (Borsa *et al.*, 1969). Thus, the elimination of NOAC is 20 times slower than that of ara-C. For the N^4-hexadecyl-ara-C derivative NHAC a similar distribution half-life $t_{1/2\alpha}$ of 16 min, but a faster elimination half-live $t_{1/2\beta}$ of 3.8 h, was determined (Horber *et al.*, 1995a). The total amount of NOAC found in blood $AUC_{(tr.\ 0\rightarrow\infty)}$ was 11% dose × h/ml and the total clearance Cl_{total} was rather low with 6 ml/h. This resulted in an apparent total volume of distribution $V_{d(area)}$ of 58 ml. The MRT was 6 h. The size of the two compartments was 10 ml for the

TABLE 1
Distribution of NOAC and NHAC in liposomes after incubation with serum and separation by gradient ultracentrifugation

Proteins	Pools Fraction nos. ($d_{20}{}^{20}$)[b]	Bound Drug per Pooled Fractions[a]			
		NOAC		NHAC	
		Liposomes	DMSO	Liposomes	DMSO
		%		%	
Albumin[c]	4–7 (1.012–1.125)	11.7±1.8	16.6±2.6	18.0±1.7	25.0±4.2
HDL	11–16 (1.102–1.074)	21.0±0.8	25.5±2.5	22.3±1.4	23.6±0.2
LDL	19–25 (1.049–1.031)	35.7±1.0	30.4±3.2	29.8±0.9	19.7±1.0
VLDL	29–50 (1.015–1.000)	4.7±0.3	5.2±0.7	3.1±0.3	3.1±0.2
Recovery		73.1±1.0	77.7±6.9	73.2±1.0	71.3±4.0

[a] Average of three experiments ± S.D.
[b] Density measured after ultracentrifugation (*cf.* fig. 3).
[c] Albumin and other serum proteins.

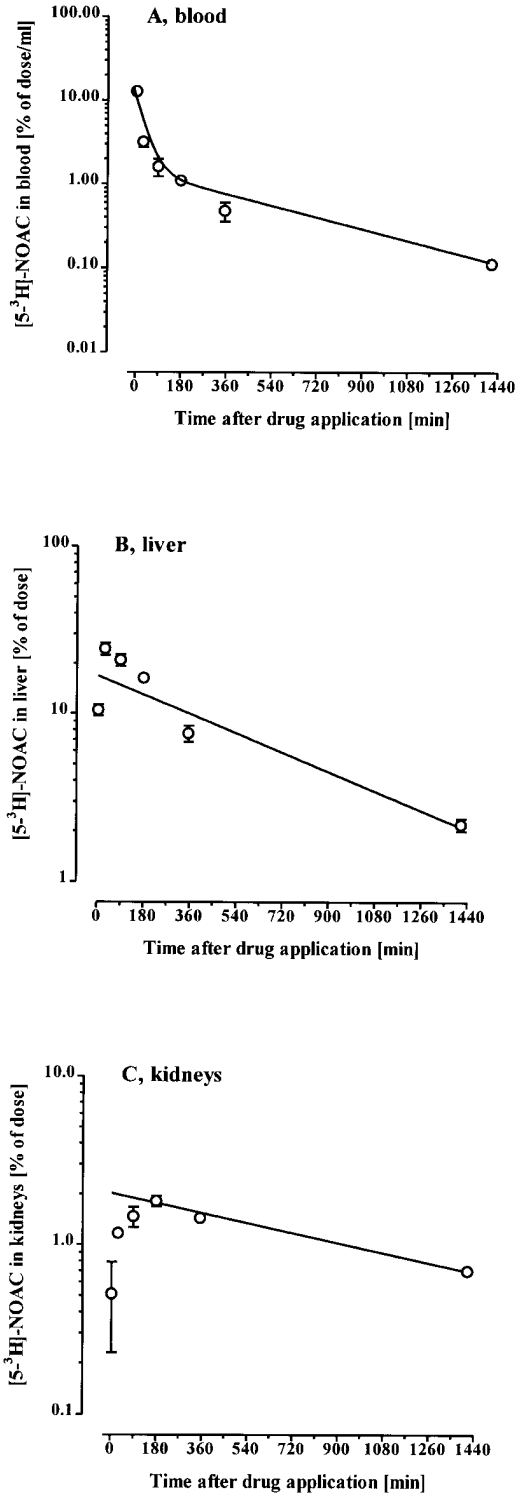

Fig. 5. Blood concentration (A), liver (B) and kidney (C) distribution *versus* time curves of NOAC (2.3 mg/animal) after i.v. application in female ICR mice. Blood samples and organs were removed and prepared for scintillation counting of [5-^{3}H]NOAC as described under "Methods." All values were standardized to a mouse body weight of 20 g and shown as percent of injected dose. Data of the blood curve (A) were fitted with the i.v. open two-compartment model, for which parameters were determined by the residual method. (Parameters: A, 9.2%/ml; B, 1.2%/ml; α, 0.0297/min; β, 0.0017/min; r, 0.934). Data for the organ curves (B, C) were fitted for the elimination phase for the liver (B, 16.9%; β, 0.0015/min; r, 0.968) and the kidneys (B, 2.0%; β, 0.00074/min; r, 0.995), respectively.

central compartment, V_c, and 33 ml for the peripheral compartment, V_p. Thus, shortly after intravenous bolus injection NOAC is distributed to other compartments. Distribution into deeper compartments occurs because $V_{d(area)}$ is 3-fold and V_p is 1.7-fold larger than the volume of total body fluids (19 ml for mice of 25 g; Allen *et al.*, 1992). Relative peak drug concentrations (table 2, figs. 5 and 6) were reached shortly after i.v. injection in blood and lung, whereas in liver and spleen they were reached after 30 min. Correspondingly, the peak concentration in the kidneys was found after 3 h. Most of the drug appears in the liver with a high organ load of 69% which can be expected for lipophilic drugs (table 2). NOAC was eliminated from the liver with a half-life of 8 h. Thus, after a single dose of NOAC more than 99% of the drug is removed from the liver within 56 h (7 times $t_{1/2\beta\ liver}$). Pharmacokinetic parameters for the brain could not be calculated because of the very low drug concentrations that were found in this organ. Distribution into the brain is quite low with less than 0.1% of the applied dose.

As summarized in table 3, the organ parameters of NOAC were calculated and compared with the data for ara-C as obtained by Nishikawa *et al.* (1993). Calculation of the organ clearance Cl_{organ} for the liver by equations 7 and 8 and standardizing the mice to a weight of 26.5 g, as used by Nishikawa *et al.* (1993), resulted in a Cl_{liver} of 2.4 ml/h. The major elimination path of NOAC is the liver comprising 55% of the total clearances, whereas the clearance from the kidneys was only 5% with a urinary clearance of 33%. The urine clearance for NOAC was calculated by use of preliminary data for cumulative drug excretion of mice kept in metabolic cages for 48 h. In comparison, 80% of ara-C were cleared through the urine (table 3).

Discussion

Binding of NOAC and NHAC to Ec. The high values of the Ec partition coefficient D_{Ec} of 3.0 and 4.2 determined for NHAC and NOAC reflect the lipophilicity of the drugs. The significantly higher affinity of NOAC for Ec might be caused by the longer alkyl chain. For comparison, Ueda and coworkers (1983) found a similarly high accumulation of N^4-behenoyl-1-β-D-arabinofuranosylcytosine in the blood cell membranes, which was significantly higher than binding to plasma proteins. This drug is a comparable lipophilic N^4-acyl-ara-C derivative. The weak binding affinity of NOAC and NHAC for Ec correlates with findings of single-chain acyl compounds like fatty acids that are not tightly anchored within lipid bilayers (Richieri *et al.*, 1993; Kleinfeld and Storch, 1993; Kamp *et al.*, 1993). In an analytical HPLC study, we observed significantly higher concentrations of the drug bound to Ec, reaching a maximal Ec-to-plasma ratio of 7:1 after 6 to 8 h, after the oral application of NOAC to mice (Rentsch *et al.*, 1995). These results are in concordance with the calculated protein binding value of 32% from the *in vitro* incubations. By extrapolation of the calculated Ec binding parameters to the average Ec concentration in a healthy human (blood volume of 4.2 liters containing 2×10^{13} Ec) and under the simplifying assumption that the Ec are the only binding partners of the drugs, saturation would be reached with a dose of 1.8 g NOAC or 2.4 g NHAC, respectively. With these drug amounts a maximal Ec binding of 0.6 g NOAC and 0.8 g NHAC would be achieved. Thus, we postulate that *in*

TABLE 2
Pharmacokinetic parameters of NOAC after intravenous application in ICR mice

Organ	Peak Concentrations		Organ Load[a]	Elimination half-time $t_{1/2\beta}$
	%[b]	min[c]	%	h
Blood	14.1 ± 0.6	4	10.8	6.9
Liver	24.4 ± 2.1	30	68.8	7.9
Spleen	0.5 ± 0.1	30	1.5	7.8
Kidneys	1.8 ± 0.1	180	14.7	16
Lung	0.9 ± 0.1	4	4.2	11
Brain	0.06 ± 0.02	4	n.d.[d]	n.d.[d]

[a] Organ $AUC_{(tr.\ 0\rightarrow\infty)}$ calculated as percent of the sum of all organ $AUC_{(tr.\ 0\rightarrow\infty)}$ values.
[b] Percentage of injected dose in total organ as means of triplicates ± S.D., standardized for mice of 20 g body weight (figs. 5 and 6).
[c] Time of the observed relative peak concentration.
[d] n.d., not determined.

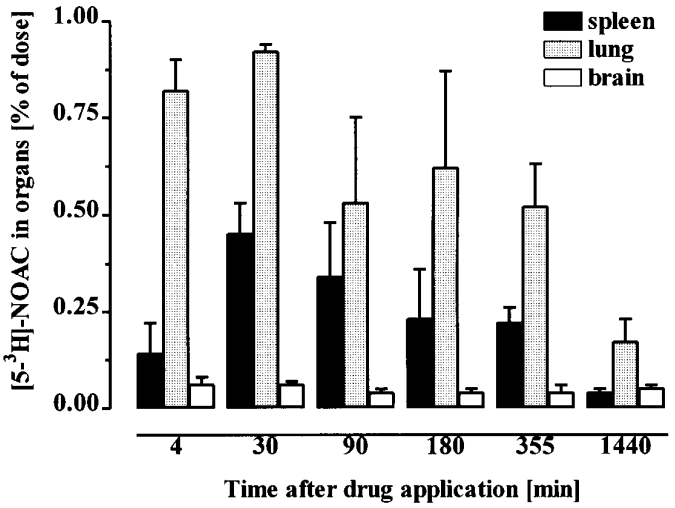

Fig. 6. Bar graph of spleen, lung and brain distribution of NOAC in female ICR mice. Data calculated as percent of injected dose were obtained after i.v. application of NOAC (2.3 mg) into the tail vein and the sacrifice of three mice at given time points. The organs were removed and prepared for counting [5-^{3}H]NOAC activity as described under "Methods."

TABLE 3
Calculation of the organ parameters for NOAC according to Nishikawa *et al.* (1993) and comparison to ara-C

Parameters[a]	NOAC		ara-C[b]	
Dose (mg/g)[c]	70 ± 10		1	
$AUC_{(0\rightarrow120\ min)}$ (%h/ml)	11[d]		3.1[e]	
	μl/h	%[f]	μl/h	%
Cl_{total}	4,400	100	28,900	100
Cl_{liver}	2,430	55	357	1.2
Cl_{spleen}	38	1	n.a.[g]	
$Cl_{kidneys}$	214	5	n.a.[g]	
Cl_{urine}	1,446[h]	33	23,000	80
Cl_{lung}	76	2	n.a.[g]	
Cl_{brain}	5	0.1	n.a.[g]	

[a] Data calculated for mice with a 26.5-g average body weight to compare values with Nishikawa *et al.* (1993) in which mice of 25–28 g were used.
[b] Data from Nishikawa *et al.* (1993).
[c] Dose per gram body weight.
[d] $AUC_{(0\rightarrow120\ min)}$ calculated from blood concentration *versus* time curve.
[e] $AUC_{(0\rightarrow120\ min)}$ calculated from plasma concentration *versus* time curve.
[f] Percent of the total clearance Cl_{total}.
[g] n.a., not analyzed.
[h] Calculated from the preliminary data of cumulative drug excretion in the urine of mice kept in metabolic cages for 48 h and determined by use of the slope of the excretion rate of the sampling period *versus* the blood concentration of NOAC.

vivo, after intravenous application of NOAC, a dynamic equilibrium between the blood components is established, favoring the initial distribution of the drug into the Ec membranes which is followed by a redistribution into the plasma proteins and preferentially into the lipoproteins. The binding of NOAC to other cells is negligible, because as we showed before with the distribution of NHAC in whole blood, only about 2% were bound to leukocytes (Horber *et al.*, 1995a).

Binding of NOAC and NHAC to serum proteins. The binding characteristics of NOAC and NHAC to the lipoproteins and mainly to LDL suggests that LDL might function as a natural carrier for these drugs. One reason for the excellent therapeutic activity of NOAC against solid tumors (Schwendener *et al.*, 1995a), which is not observed with ara-C, might be explained by its high affinity to LDL (fig. 3, table 1) and its postulated carrier effect on tumor cells expressing high numbers of LDL receptors. Other investigators (de Smidt *et al.*, 1993; de Smidt and van Berkel, 1990) exploited this LDL carrier effect for selective drug targeting to tumor cells with high-LDL receptor expression. Vitols *et al.* (1990) observed an increased uptake with radioactively labeled sucrose-LDL in leukocytes of leukemic patients, which suggested a correlation to the increased LDL receptor activity of leukemic compared with normal leukocytes. Finally, lipophilic photosensitizer dyes were found to be associated with lipoproteins and transported mainly by LDL to malignant cells (Ginevra *et al.*, 1990; Reddi *et al.*, 1990; Rensen *et al.*, 1994; Schmidt-Erfurth *et al.*, 1997). Therefore, LDL might be an efficient carrier for various drugs to treat leukemias and solid tumors with increased LDL turnover, *e.g.*, metastatic cancer of the prostate as described by Vitols *et al.* (1990). Firestone (1994) reported that there are several types of carcinoma cells with an increased LDL uptake, especially tumor cells that have an exceptionally high metastatic potential, or that are aggressive or undifferentiated. The rationale is that large amounts of LDL are taken up by rapidly dividing cells because an increased amount of cholesterol is required for cell membrane assembly. However, the use of LDL as a carrier for lipophilic drugs is limited by complicated procedures required for its isolation from human serum and its modification as a drug transporter molecule (Firestone, 1994; Gerke *et al.*, 1996). These and other disadvantages, such as the ensuing risk of infection of LDL isolated from human blood, render the clinical use of LDL as a drug carrier for cancer therapies rather unlikely. We found that after incubation in serum 30 to 36% of NOAC molecules were bound to LDL. The serum volume of 1 ml contains approximately 5.5×10^{14} LDL particles as determined and calculated by quantitative agarose gel electrophoresis (Hydragel,

Sebia, Issy-les-Moulineaux, France; data not shown). Thus, we calculated that one LDL particle is able to bind about 100 molecules of NOAC.

The rapid transfer of NOAC from the liposome membranes to Ec and the lipoproteins demonstrates that the liposomes serve mainly as a pharmaceutical formulation to enable the parenteral application of these lipophilic drugs and that their influence on the pharmacokinetic parameters of the drugs is marginal and probably occurs only shortly after drug injection. In another study we demonstrated that NHAC formulated in long-circulating poly(ethylene glycol)-modified liposomes (PEG-liposomes, Stealth liposomes) was distributed at comparable rates to blood components as with unmodified liposomes (Horber *et al.*, 1995a), demonstrating that the modified surface of the PEG-liposomes did not prevent the transfer of the liposome membrane-associated drug to Ec and lipoproteins. Furthermore, the antitumor activity of both ara-C derivatives in PEG-liposomes was not significantly improved in the L1210 mouse leukemia model compared with drug formulations without PEG-modified liposomes (Schwendener *et al.*, 1995b), which also suggests that the antitumor activity of the drugs does not depend on the liposome composition.

Pharmacokinetics of NOAC in mice. Liposomes are generally used to improve the blood pharmacokinetics of encapsulated hydrophilic drugs like ara-C (Allen *et al.*, 1992) or doxorubicin (Vaage *et al.*, 1994) that have short plasma half-lives when administered in their free form. Ara-C encapsulated within long-circulating liposomes remains in the circulation because Allen *et al.* (1992) determined a distribution volume V_d of 2.2 ml (= blood volume). Compared with free ara-C which is distributed in the total body fluid (V_d = 19 ml), the distribution volume of NOAC $V_{d(area)}$ of 58 ml is about three times larger, which indicates the distribution into deeper compartments that might be caused by the high lipophilicity of NOAC.

The further comparison of the pharmacokinetic parameters of NOAC with those reported by Nishikawa *et al.* (1993) for ara-C (table 3) revealed that NOAC is eliminated by urine and through the liver, whereas ara-C is excreted mainly in urine. Additionally, the kidney load of 15% suggests that some of the drug or its metabolites are removed from circulation by this organ. It is more likely that hydrophilic metabolites of NOAC are cleared by the kidneys, which is in accordance with the late peak concentration of 3 h and the high renal elimination half-life of 16 h. To confirm our findings that NOAC and metabolites are excreted by the kidneys and through the bile we performed the above-mentioned preliminary experiment in which urine and feces were collected during a 48-h period. As expected, we found radioactivity in both elimination paths, namely 38% of the injected tritium activity in the urine and 25% in the feces. Presently, we are performing an analysis of the metabolites of NOAC from liver homogenates, urine and fecal extracts by HPLC-mass spectroscopy. From the ongoing clinical phase I/II study in cancer patients with liposomal NOAC, we determined the plasma half-lives of the first two dosages given. At the dosages of 150 and 300 mg NOAC/m^2, a $t_{1/2\alpha}$ of 14 min and a $t_{1/2\beta}$ of 11 to 16 h and peak drug concentrations of 13 to 37 μM were calculated.

In this report we demonstrated that NOAC behaves pharmacokinetically different from ara-C and that its affinity to LDL might prove to be a promising advantage in tumor therapy.

Acknowledgment

The authors would like to thank K. M. Rentsch and D. Horber for their assistance.

References

Allen, T. M.: Stealth-liposomes: Avoiding reticuloendothelial uptake. *In* Liposomes in the Therapy of Infectious Diseases and Cancer, ed. by G. Lopez-Berenstein and I. J. Fidler, pp. 405–415, Alan R. Liss, New York, 1989.

Allen, T. M., Mehra, T., Hansen, C. and Chin, Y. C.: Stealth liposomes: an improved sustained release system for 1-β-D-arabinofuranosylcytosine. Cancer Res. **52:** 2431–2439, 1992.

Aoshima, M., Tsukagoshi, S., Sakurai, Y., Oh Ishi, J. and Ishida, T.: Antitumor activities of newly synthesized N^4-acyl-1-β-D-arabinofuranosylcytosine. Cancer Res. **36:** 2726–2732, 1976.

Borsa, J., Whitmore, G. R., Valeriote, F. A., Collins, D. and Bruce, W. R.: Studies on the persistence of methotrexate, cytosine arabinoside, and leucovorin in the serum of mice. J. Natl. Cancer Inst. **42:** 235–242, 1969.

Chapman, M. J., Goldstein, S., Lagrange, D. and Laplaud, P. M.: A density gradient ultracentrifugal procedure for the isolation of the major lipoprotein classes from human serum. J. Lipid Res. **22:** 339–358, 1981.

De Smidt, P. C. and Van Berkel, T. J. C.: Prolonged serum half-life of antineoplastic drugs by incorporation into the low density lipoprotein. Cancer Res. **50:** 7476–7482, 1990.

De Smidt, P. C., Versluis, A. J. and Van Berkel, T. J.: Properties of incorporation, redistribution, and integrity of porphyrin-low-density lipoprotein complexes. Biochemistry **32:** 2916–2922, 1993.

Derendorf, H. and Garrett, E. R.: High-performance liquid chromatographic assay of methadone, phencyclidine, and metabolites by postcolumn ion-pair extraction and on-line fluorescent detection of the counterion with applications. J. Pharm. Sci. **72:** 630–635, 1983.

Firestone, R. A.: Low-density lipoprotein as a vehicle for targeting antitumor compounds to cancer cells. Bioconjug. Chem. **5:** 105–113, 1994.

Gahrton, G.: Treatment of acute leukemia: Advances in chemotherapy, immunotherapy and bone marrow transplantation. Adv. Cancer Res. **40:** 255–329, 1983.

Gerke, A., Westensen, K. and Koch, M. H. J.: Physicochemical characterization of protein-free low density lipoprotein models and influence of drug loading. Pharm. Res. **13:** 44–51, 1996.

Ginevra, F., Biffanti, S., Pagnan, A., Biolo, R., Reddi, E. and Jori, G.: Delivery of the tumour photosensitizer zinc(II)-phthalocyanine to serum proteins by different liposomes: Studies in vitro and in vivo. Cancer Lett. **49:** 59–65, 1990.

Greenblatt, D. J. and Koch-Weser, J.: Clinical pharmacokinetics (first of two parts). N. Engl. J. Med. **2:** 702–705, 1975.

Ho, D. H. and Frei, E., III: Clinical pharmacology of 1-β-D-arabinofuranosyl cytosine. Clin. Pharmacol. Ther. **12:** 944–954, 1971.

Hope, M. J., Bally, M. B., Webb, G. and Cullis, P. R.: Production of large unilamellar vesicles by a rapid procedure, characterization of size distribution, trapped volume and ability to maintain a membrane potential. Biochim. Biophys. Acta **812:** 55–65, 1985.

Horber, D. H., Ottiger, C., Schott, H. and Schwendener, R. A.: Pharmacokinetic properties and interactions with blood components of N^4-1-β-D-arabinofuranosylcytosine (NHAC) incorporated into liposomes. J. Pharm. Pharmacol. **47:** 282–288, 1995a.

Horber, D. H., Schott, H. and Schwendener, R. A.: Cellular pharmacology of a liposomal preparation of N^4-hexadecyl-1-β-D-arabinofuranosylcytosine, a lipophilic derivative of 1-β-D-arabinofuranosylcytosine. Br. J. Cancer **71:** 957–962, 1995b.

Horber, D. H., Schott, H. and Schwendener, R. A.: Cellular pharmacology of N^4-hexadecyl-1-β-D-arabinofuranosylcytosine in the human leukemic cell lines K-562 and U-937. Cancer Chemother. Pharmacol. **36:** 483–492, 1995c.

Horber, D. H., Von Ballmoos, P., Schott, H. and Schwendener, R. A.: Cell cycle-dependent cytotoxicity and induction of apoptosis by liposomal N^4-hexadecyl-1-β-D-arabinofuranosylcytosine. Br. J. Cancer **72:** 1067–1073, 1995d.

Kamp, F., Hamilton, J. A. and Westerhoff, H. V.: Movement of fatty acids, fatty acid analogues, and bile acids across phospholipid bilayers. Biochemistry **32:** 11074–11086, 1993.

Kanai, T. and Ichino, M.: Pyrimidine nucleosides. 6. Syntheses and anticancer activities of N^4-substituted 2,2′-anhydronucleosides. J. Med. Chem. **17:** 1076–1078, 1974.

Kataoka, T. and Sakurai, Y.: Effect and mode of action of N^4-behenoyl-β-D-arabinofuranosylcytosine. Recent Results. Cancer Res. **70:** 147–151, 1980.

Keating, M. J., McCredie, K. B., Bodey, G. P., Smith, T. L., Gehan, E. and Freireich, E. J.: Improved prospects for long-term survival in adults with acute myelogenous leukemia. JAMA **248:** 2481–2486, 1982.

Kleinfeld, A. M. and Storch, J.: Transfer of long-chain fluorescent fatty acids between small and large unilamellar vesicles. Biochemistry **32:** 2053–2061, 1993.

Nishikawa, M., Kamijo, A., Fujita, T., Takakura, Y., Sezaki, H. and Hashida, M.: Synthesis and pharmacokinetics of a new liver-specific carrier, glycosylated carboxymethyl-dextran, and its application to drug targeting. Pharm. Res. **10:** 1253–1261, 1993.

Noble, R. P.: Electrophoretic separation of plasma lipoproteins in agarose gel. J. Lipid Res. **9:** 693–700, 1968.

Plunkett, W. and Gandhi, V.: Cellular pharmacodynamics of anticancer drugs. Semin. Oncol. **20:** 50–63, 1993.

Reddi, E., Zhou, C., Biolo, R., Menegaldo, E. and Jori, G.: Liposome- or LDL-administered Zn (II)-phthalocyanine as a photodynamic agent for tumours. I. Pharmacokinetic properties and phototherapeutic efficiency. Br. J. Cancer **61:** 407–411, 1990.

Redgrave, T. G., Roberts, D. C. K. and West, C. E.: Separation of plasma lipoproteins by density-gradient ultracentrifugation. Anal. Biochem. **65:** 42–49, 1975.

Rensen, P. C., Love, W. G. and Taylor, P. W.: In vitro interaction of zinc(II)-phthalocyanine-containing liposomes and plasma lipoproteins. J. Photochem. Photobiol. B **26:** 29–35, 1994.

Rentsch, K. M., Schwendener, R. A., Schott, H. and Hänseler, E.: Sensitive high-performance liquid chromatographic method for the determination of N^4-hexadecyl- and N^4-octadecyl-1-β-D-arabinofuranosylcytosine in plasma and erythrocytes. J. Chromatogr. B **673:** 259–266, 1995.

Richieri, G. V., Anel, A. and Kleinfeld, A. M.: Interactions of long-chain fatty acids and albumin: Determination of free fatty acid levels using the fluorescent probe ADIFAB. Biochemistry **32:** 7574–7580, 1993.

Rosowsky, A., Kim, S. H., Ross, J. and Wick, M. M.: Lipophilic 5′-(alkyl phosphate) esters of 1-β-D-arabinofuranosylcytosine and its N^4-acyl and 2,2′-anhydro-3′-O-acyl derivatives as potential prodrugs. J. Med. Chem. **25:** 171–178, 1982.

Rubas, W., Supersaxo, A., Weder, H. G., Hartmann, H. R., Hengartner, H., Schott, H. and Schwendener, R.: Treatment of murine L1210 lymphoid leukemia and melanoma B16 with lipophilic cytosine arabinoside prodrugs incorporated into unilamellar liposomes. Int. J. Cancer **37:** 149–154, 1986.

Schmidt-Erfurth, U., Diddens, H., Birngruber, R. and Hasan, T.: Photodynamic targeting of human retinoblastoma cells using covalent low-density lipoprotein conjugates. Br. J. Cancer **75:** 54–61, 1997.

Schwendener, R. A., Horber, D. H., Odermatt, B. and Schott, H.: Oral antitumour activity in murine L1210 leukaemia and pharmacological properties of liposome formulations of N^4-alkyl derivatives of 1-β-D-arabinofuranosylcytosine. J. Cancer Res. Clin. Oncol. **122:** 102–108, 1996.

Schwendener, R. A., Horber, D. H., Ottiger, C., Rentsch, K. M., Fiebig, H. H. and Schott, H.: Alkasar-18, 1-(β-D-arabinofuranosyl)-4-octadecylamino-2(1H)-pyrimidin-one, N^4-octadecyl-ara-C, NOAC. Drugs Future **20:** 11–15, 1995a.

Schwendener, R. A., Horber, D. H., Ottiger, C. and Schott, H.: Preclinical properties of N^4-hexadecyl- and N^4-octadecyl-1-β-D-arabinofuranosylcytosine in liposomal preparations. J. Liposome Res. **5:** 27–47, 1995b.

Schwendener, R. A. and Schott, H.: Treatment of L1210 murine leukemia with liposome incorporated N^4-hexadecyl-1-β-D-arabinofuranosylcytosine. Int. J. Cancer **51:** 466–469, 1992.

Schwendener, R. A. and Schott, H.: Lipophilic 1-β-D-arabinofuranosylcytosine (Ara-C) derivatives in liposomal formulations for the oral and parenteral antileukemic therapy in the murine L1210 leukemia model. J. Cancer Res. Clin. Oncol. **122:** 723–726, 1996.

Tsuruo, T., Tsukagoshi, S. and Sakurai, Y.: N^4-palmitoyl- and N^4-stearoyl-1-β-D-arabinofuranosylcytosine as new antitumor agent. *In* Current Chemotherapy and Infections Disease, ed. by J. D. Grassi, pp. 1591–1593, The American Society of Microbiology, Washington, DC, 1980.

Ueda, T., Nakamura, T., Ando, S., Kagawa, D., Sasada, M., Uchino, H., Johno, I. and Akiyama, Y.: Pharmacokinetics of N^4-behenoyl-1-β-D-arabinofuranosylcytosine in patients with acute leukemia. Cancer Res. **43:** 3412–3416, 1983.

Vaage, J., Barbera Guillem, E., Abra, R., Huang, A. and Working, P.: Tissue distribution and therapeutic effect of intravenous free or encapsulated liposomal doxorubicin on human prostate carcinoma xenografts. Cancer **73:** 1478–1484, 1994.

Vitols, S., Angelin, B., Ericsson, S., Gahrton, G., Juliusson, G., Masquelier, M., Paul, C., Peterson, C., Rudling, M., Soderberg Reid, K. and Tidefelt, U.: Uptake of low density lipoproteins by human leukemic cells in vivo: relation to plasma lipoprotein levels and possible relevance for selective chemotherapy. Proc. Natl. Acad. Sci. U.S.A. **87:** 2598–2602, 1990.

Wempen, I., Miller, N., Falco, E. A. and Fox, J. J.: Nucleosides. XLVII. Synthesis of some N^4-substituted derivatives of 1-β-D-arabinofuranosylcytosine and -5-5-fluorocytosine. J. Med. Chem. **11:** 144–148, 1968.

Send reprint requests to: Reto A. Schwendener, Ph.D., Department of Pathology, Division of Cancer Research, University Hospital, Schmelzbergstrasse 12, CH-8091 Zürich, Switzerland.